Supramolecular architecture of endoplasmic reticulum - plasma membrane contact sites

Rubén Fernández-Busnadiego

Department of Molecular Structural Biology, Max Planck Institute of Biochemistry

Am Klopferspitz 18, 82152 Martinsried, Germany

Correspondence to: ruben@biochem.mpg.de

Summary

The endoplasmic reticulum (ER) forms membrane contact sites (MCS) with most other cellular organelles and the plasma membrane (PM). These ER-PM MCS, where the membranes of the ER and PM are closely apposed, were discovered in the early days of electron microscopy (EM), but only recently are we starting to understand their functional and structural diversity. ER-PM MCS are nowadays known to mediate excitation-contraction coupling in striated muscle cells and to play crucial roles in Ca^{2+} and lipid homeostasis in all metazoan cells. A common feature across ER-PM MCS specialized in different functions is the preponderance of cooperative phenomena that result in the formation of large supramolecular assemblies. Therefore, characterizing the supramolecular architecture of ER-PM MCS is critical to understand their mechanisms of function. Cryo-electron tomography (cryo-ET) is a powerful EM technique uniquely positioned to address this issue, as it allows 3D imaging of fully hydrated, unstained cellular structures at molecular resolution. In this review I summarize our current structural knowledge on the molecular organization of ER-PM MCS and its functional implications, with special emphasis on the emerging contributions of cryo-ET.

Keywords

Ryanodine receptor, STIM, Orai, Extended-synaptotagmin, lipid transfer, cryo-EM

Introduction

Compartmentalization into different membrane-bound organelles provides great versatility to eukaryotic cells by enabling a wide diversity of biochemical reactions. However, like the members of an orchestra, cellular compartments need to communicate with each other to play at unison. The importance of membrane traffic and signaling cascades in this communication is well established, but recent research is starting to highlight another major player: inter-organellar communication at membrane contact sites (MCS). MCS are regions of close (~ 20 nm) apposition between two cellular membranes that play central roles in lipid metabolism, Ca^{2+} homeostasis and other fundamental cellular processes. Most organelles are nowadays known to engage in MCS, but perhaps none of them to the extent of the ER. The ER forms MCS with virtually all other organelles, including the Golgi apparatus, mitochondria, lysosomes or endosomes. The ER also establishes MCS with the PM, whose structure and molecular organization will be the focus of this review. The reader is referred to excellent recent reviews on other aspects of ER-PM MCS or MCS between other cellular membranes [1-5].

EM has been of pivotal importance in the discovery and understanding of MCS function. ER-PM MCS were first observed in the early days of cellular electron microscopy (Fig. 1A) [6], and the first

systematic structural characterization of such “subsurface cisterns” was carried out only a few years later (Fig. 1B) [7]. Soon after, conclusive EM evidence demonstrated that the triad junctions of muscle cells were also a specialized ER-PM MCS that mediated the excitation-contraction coupling [8]. The functions of ER-PM MCS in non-muscle cells remained enigmatic until the last decade, when the discovery of the STIM/Orai system revealed that ER-PM MCS mediate store-operated Ca^{2+} entry (SOCE) in all metazoan cells. More recently, ER-PM MCS have been shown to play critical roles in signaling and lipid metabolism and exchange between bilayers. Extensive research has identified many of the key molecular players of these processes and the list is rapidly growing. It is now clear that cooperative phenomena involving the formation of large homo and heteromeric assemblies lay at the heart of ER-PM MCS function, making of the utmost importance to understand how these supramolecular structures are built and organized within the narrow space between the ER and the PM. Several laboratories have successfully tackled this challenge using a variety of biochemical or light microscopy approaches, but recent technical advances are bringing about a renaissance of EM as a powerful tool to study MCS architecture. In particular, cryo-electron tomography (cryo-ET) enables 3D imaging of unstained biological structures exquisitely preserved by vitrification within the native context of intact cells and at molecular resolution [9]. In this review I will summarize the current knowledge on the molecular architecture of the main categories of ER-PM MCS known to date, highlighting the contributions of last generation EM techniques.

ER-PM MCS in striated muscle

ER-PM MCS in striated muscle are perhaps the MCS of most distinct architecture and thus historically the first studied in detail [8, 10]. These junctions are formed between a PM specialization known as the T-tubule and the sarcoplasmic reticulum (SR, a special type of ER found in muscle cells). In cardiac muscle a single SR terminal cisterna contacts the T-tubule forming a structure known as dyad, whereas in skeletal muscle two SR terminal cisternae contacting a T-tubule form the so-called triads. In both types of junctions L-type Ca^{2+} channels (also known as dihydropyrine receptors, DHPR) on the T-tubule closely associate with ryanodine receptors (RyR) on the SR membrane to mediate the excitation-contraction coupling (ECC). In brief, a nervous signal triggers depolarization of the PM of the muscle cell, thereby activating Ca^{2+} influx through DHPR. This modest influx of extracellular Ca^{2+} triggers massive release of Ca^{2+} from SR stores through RyRs, which in turn activates the actin/myosin machinery to drive muscle contraction [11, 12].

The DHPR-RyR couplon is an excellent example of the importance of supramolecular architecture for MCS function. DHPRs assemble into groups of four (“tetrads”) that associate closely with the four-fold symmetric RyRs [13, 14]. This is important to allow the formation of Ca^{2+} nanodomains, in which a relatively small influx of extracellular Ca^{2+} through DHPRs may reach sufficient intracellular concentrations to activate RyRs [12, 15]. The physical proximity between DHPRs and RyRs also allows Ca^{2+} released by RyR to mediate the Ca^{2+}-dependent inactivation of DHPR [16] and, in skeletal muscle, enables physical DHPR-RyR interactions by which DHPR modulate RyR function [15, 17]. Similar Ca^{2+} nanodomains formed by the spatial coupling of Ca^{2+} channels and their downstream effectors underlie other fundamental biological processes such as neurotransmitter release, the excitation-transcription coupling or Ca^{2+}-dependent enzyme activation [18-20]. Interestingly, recent research implicates RyRs in the establishment of Ca^{2+} nanodomains at other MCS, such as those formed by the SR/ER and mitochondria in cardiomyocytes and pancreatic beta cells [15].

Consequently, the regulation of the distance between SR and T-tubule membranes is of critical importance. This distance is mainly controlled by junctophilins, which function as tethers by inserting in the SR membrane through a C-terminal transmembrane segment and binding the T-tubule via their N-terminal membrane occupation and recognition nexus sequences. Deletion of the heart-specific

isoform junctophilin 2 results in increased intermembrane distance and embryonic mortality [21]. Rather than mere spacers, junctophilins seem to directly link DHPRs and RyRs to position them opposite to each other and ensure efficient ECC [22]. At the same time, additional cytosolic binding partners such as calmodulin or FKBP12/calstabin1 and a large SR luminal complex formed by calsequestrin, junctin, triadin and others regulate the Ca^{2+} release properties of RyRs [11]. Furthermore, theoretical and experimental evidence has shown that the spatial relationship between neighboring DPHR-RyR couplons plays a major role in ECC [12, 23]. These couplons assemble into clusters containing a few units in cardiac muscle and much larger checkerboard patterns in skeletal muscle (Fig. 1C) [24-26].

The large size of the cytosolic portion of the RyR (~ 30 nm in diameter) [14] has facilitated the study of these clustering phenomena by sub-diffraction light microscopy techniques, which achieve resolutions close to the size of individual receptors. Nevertheless, most of the information available to date on the molecular architecture of ER-PM MCS in muscle has been provided by thin section and freeze-fracture EM work [13]. Visualization of components of the junction smaller than RyRs or DHPRs has been hindered by technical limitations, but pioneering cryo-ET work tackled this issue in fully hydrated, unstained isolated triad junctions [27, 28]. These studies measured an average separation between SR and T-tubule membranes of 15.5 ± 1 nm and, coupled with sub-tomogram averaging, hinted to a periodic arrangement of the calsequestrin layer, which is separated from the RyRs by a 5 nm gap bridged by fine filaments that could correspond to proteins such as triadin or junctin. Altogether, the work summarized here shows that the function of ER-PM MCS in muscle is exquisitely determined by their molecular architecture.

Store-operated Ca^{2+} entry

Research from the last ten years demonstrated that the integral ER membrane protein stromal-interacting molecule (STIM) and the PM Orai Ca^{2+} channels mediate the long sought mechanism for SOCE [4]. As the SR in muscle, the ER is the major intracellular Ca^{2+} store in all metazoan non-muscle cells. ER Ca^{2+} is released in a variety of signaling processes, often as a result of the receptor-mediated activation of phospholipase C, which hydrolyzes PM phosphatidylinositol 4,5-bisphosphate ($PI(4, 5)P_2$) to produce inositol trisphosphate (IP_3) that in turn activates Ca^{2+} release from the ER via IP_3-receptor Ca^{2+} channels on the ER membrane. To sustain signaling, ER Ca^{2+} is refilled by SOCE through a series of major conformational changes, as revealed by a combination of structural approaches including Förster resonance energy transfer, NMR and X-ray crystallography [29]. At rest, STIM molecules likely form dimers on the ER membrane. Upon store depletion low ER Ca^{2+} levels result in Ca^{2+} dissociation from the EF hands in the luminal domain of STIM and trigger STIM oligomerization via its luminal sterile α-motif. STIM oligomers extend their coil-coiled domains to adopt an elongated conformation that reaches over to bind Orai Ca^{2+} channels at the PM, thereby activating Ca^{2+} influx into the cell and recruiting further Orai channels to form large STIM/Orai assemblies. The exact stoichiometry of single STIM/Orai complexes is still debated, but diffusion trapping experiments and the hexameric arrangement of Orai revealed by its X-ray structure suggest that one or two STIM dimers could suffice to immobilize one Orai molecule at ER-PM MCS. Finally, sarco/endoplasmic reticulum Ca^{2+}-ATPases pump Ca^{2+} into the ER lumen to maintain ER Ca^{2+} homeostasis. This process is further regulated by a long and possibly yet incomplete list of interactors, which includes septins, junctate, CRACR2A, α-SNAP, SARAF and STIMATE [30].

Just as in DHPR-RyR-mediated ER-PM MCS in muscle, the architecture of STIM/Orai MCS defines the Ca^{2+} signaling properties of these junctions [31]. ER-PM distance is perhaps the most fundamental geometrical constraint, but diverging values for this distance at STIM/Orai MCS formed in different mammalian cells upon STIM1 overexpression have been reported in the EM literature, ranging from 8

to 17 nm with individual distances as short as 1 nm [32, 33]. However, these numbers must be treated with caution given the unavoidable shrinkage of dehydrated material and that the distances were measured between the layers of heavy metal stain covering the membranes rather than between the membranes themselves. We have recently used cryo-ET to study ER-PM MCS formed by stimulation of the muscarinic receptor M1R in fully hydrated, unstained cells overexpressing STIM1 [34]. Under these conditions the average ER-PM distance was 21.1 ± 1.3 nm (mean ± SEM), slightly shorter than that observed in untransfected neurons (23.3 ± 1.2 nm, mean ± SEM) arguing against major spurious influence of STIM1 overexpression in ER-PM distance. As no staining was used, this distance directly reflects the separation between the phospholipid head groups on both membranes. Our data also revealed filamentous densities bridging the gap between the ER and the PM roughly perpendicular to both membranes (Fig. 2A, B), and these filaments were often clustered in groups and/or connected to large ER luminal or extracellular densities. Even though a high resolution structure of full length STIM1 is not yet available, the morphology of these filaments is consistent with structural models of activated STIM1, whose cytosolic region contains long presumably unstructured sequences and coil coiled domains that alone could reach at least 15 nm in their extended conformation [4]. Thus, it is likely that the filamentous structures observed by cryo-ET provide a first glimpse onto the complex formed by Orai, STIM and their interactors in situ, paving the way for more detailed future studies.

Lipid exchange at ER-PM MCS

Besides their roles in Ca^{2+} signaling and homeostasis, ER-PM MCS are emerging as important hubs for lipid metabolism and exchange between membranes. The ER is the major site of lipid synthesis in the cell, but for a long time it was thought that the only substantial mechanism of ER lipid delivery to the PM was vesicular traffic via the Golgi apparatus. However, recent work has shown that several proteins directly shuttle lipids between the ER and plasma membranes at MCS. In particular, ORP (oxysterol-binding protein [OSBP]-related protein)/Osh (oxysterol-binding homology) proteins are major lipid transporters between the ER and other cellular membranes, including the PM [35]. OSBP, the founding member of the family, countertransports sterols and phosphatidylinositol 4-phosphate (PI4P) at ER-Golgi MCS [36]. Similarly, ORP5/8 in mammals and Osh6/7 in yeast exchange phosphatidylserine and PI4P at ER-PM MCS [37, 38]. Osh3 regulates PM phosphoinositide (PI) metabolism at ER-PM MCS, either by PI4P countertransport with another lipid or by directly modulating the enzymatic activity of the PI phosphatase Sac 1 on the ER membrane [39]. In addition to ORP/Osh proteins, Nir2 shuttles phosphatidylinositol from the ER to the PM to help maintaining PM PI(4, 5)P_2 levels [40].

ORP/Osh proteins play additional structural roles as ER-PM tethers, as they bind PM PI4P via their pleckstrin homology domains and the ER either by hydrophobic tail sequences or by interacting with ER-resident Scs/VAP (VAMP-associated protein) [36, 38, 39]. However, other ER-PM tethers exist. In yeast around 40% of the PM surface is engaged in MCS with the ER, but simultaneous deletion of six proteins (Tricalbins 1/2/3, the VAP proteins Scs2 and Scs22 and Ist2) practically abolishes these contacts [41]. The family of Extended-Synaptotagmins (E-Syts) are the mammalian the homologs of the tricalbins and contain an SMP (synaptotagmin-like mitochondrial-lipid-binding protein) domain and three (E-Syt2/3) or five (E-Syt1) C2 domains. E-Syts tether the ER to the PM, as they are anchored to the ER membrane by a hairpin sequence and bind PM PI(4, 5)P_2 by a basic patch in their C-terminal C2 domains [34, 42, 43]. Additionally, the C2C domain of E-Syt1 binds PM PI(4, 5)P_2 in a Ca^{2+}-dependent manner, and E-Syt1 confers Ca^{2+} sensitivity to E-Syt2/3 by the formation of heterodimers. E-Syts may also be implicated in lipid transfer, as their SMP domain forms a head-to-head dimer creating a hydrophobic groove that harbors lipids [44]. Interestingly, SMP domains have so far only been found in MCS-resident proteins [45].

How the E-Syts and other tethering or lipid transfer proteins are organized at ER-PM MCS remains unknown. We have recently employed cryo-ET to show that in E-Syt-mediated ER-PM MCS an electron dense layer runs parallel to the membranes at a distance of approximately 8 nm from the ER membrane, in stark structural contrast with the filaments observed in STIM1/Orai-mediated contacts (Fig. 2D, E) [34]. Interestingly, this intermediate density covers extended portions of the ER-PM MCS surface, indicating that it is formed by large oligomeric entities across the whole junction, at least under conditions of E-Syt overexpression. Given that the morphology of this intermediate density was similar in E-Syt1- and E-Syt3-mediated ER-PM MCS, such supramolecular assembly may be formed by the domains shared by these E-Syts (SMP, C2A and C2B) plus perhaps some interactors of those domains. The respective distances between ER and PM in E-Syt3- and E-Syt1-mediated ER-PM MCS were 18.8 ± 0.4 nm and 21.8 ± 1.8 nm (mean ± SEM), likely reflecting the additional two C2 domains of E-Syt1 versus E-Syt3. Increased concentrations of cytosolic Ca^{2+} in E-Syt1-mediated MCS resulted in a dramatic shortening of the ER-PM distance to 14.8 ± 1.1 nm (mean ± SEM), probably mediated by the Ca^{2+}-dependent binding of E-Syt1 C2C domain to PM PI(4, 5)P_2 (Fig. 2F). It is likely that this Ca^{2+}-dependent regulation of ER-PM distance has profound implications on intermembrane lipid exchange mediated either directly by E-Syts or by other ER-PM MCS-resident proteins such as Nir2 [40]. In the light of the high resolution protein structures known to date and given that ER-PM distances are rarely shorter than 10 nm, our data also suggest that lipid shuttling between membranes might be a more plausible mechanism of transfer than direct tunneling by proteins contacting both bilayers simultaneously. Thus, as the architecture of ER-PM MCS is fundamental to define the properties of Ca^{2+} nanodomains, it is also a crucial regulator of lipid transfer at these membrane junctions.

Conclusions and perspectives

A common theme to the different aspects of ER-PM MCS function are cooperative phenomena that result in the formation of large macromolecular assemblies of poorly understood stoichiometry, such as clusters of DHPR-RyR couplons, STIM and Orai Ca^{2+} channels or the density layer across E-Syt-mediated contacts. The temporal dynamics of these assemblies are heterogeneous, since ER-PM MCS are very stable in muscle but rearrange rapidly in the case of STIM/Orai- and E-Syt-mediated MCS. The picture is yet more complex, because different categories of ER-PM MCS-resident proteins may coexist at the same junction. For example, not only SOCE plays an important role in SR Ca^{2+} replenishment in muscle, but STIM1 also interacts directly with DHPRs and regulates their activity [46]. Also, E-Syt1 and STIM1 are recruited to the same ER-PM MCS upon induction of SOCE and E-Syt1 is involved in the Ca^{2+}-dependent inactivation of SOCE mediated by SARAF [42, 47]. Our cryo-ET observations of ER-PM MCS in untransfected neurons also support the notion that multiple types of tethers coexist at native MCS (Fig. 2C) [34]. A multidisciplinary approach will be necessary to tackle this complexity and determine the precise molecular architecture of ER-PM MCS. In particular, the combination of cryo-ET with recent technological advances such as cryo-focused ion beam milling, Volta phase plates and direct electron detectors [9, 48] as well as other techniques such as super-resolution light microscopy [23] has an unparalleled potential to reveal the structural and functional underpinnings of MCS at molecular resolution.

Acknowledgments

I wish to thank Eri Sakata, Francesca Giordano, Chris Stefan and Pietro De Camilli for the critical reading of this manuscript, and Monika Krause for graphical assistance with Figure 2F. I apologize to the authors of primary work that were not cited due to space limitations.

Funding

R. F.-B. is supported by the FP7 GA ERC-2012-SyG_318987–ToPAG grant from the European Commission.

Abbreviations

Cryo-ET: cryo-electron tomography

DHPR: dihydropyrine receptor

E-Syt: extended-synaptotagmin

ECC: excitation-contraction coupling

EM: electron microscopy

ER: endoplasmic reticulum

IP_3: inositol trisphosphate

MCS: membrane contact site

ORP: oxysterol-binding protein-related protein

OSBP: oxysterol-binding protein

Osh: oxysterol-binding homology

PI: phosphoinositide

PI4P: phosphatidylinositol 4-phosphate

PI(4, 5)P_2: phosphatidylinositol 4,5-bisphosphate

PM: plasma membrane

RyR: ryanodine receptor

SMP: synaptotagmin-like mitochondrial-lipid-binding protein

SOCE: store-operated Ca^{2+} entry

SR: sarcoplasmic reticulum

STIM: stromal-interacting molecule

VAP: VAMP-associated protein

Figures

Figure 1

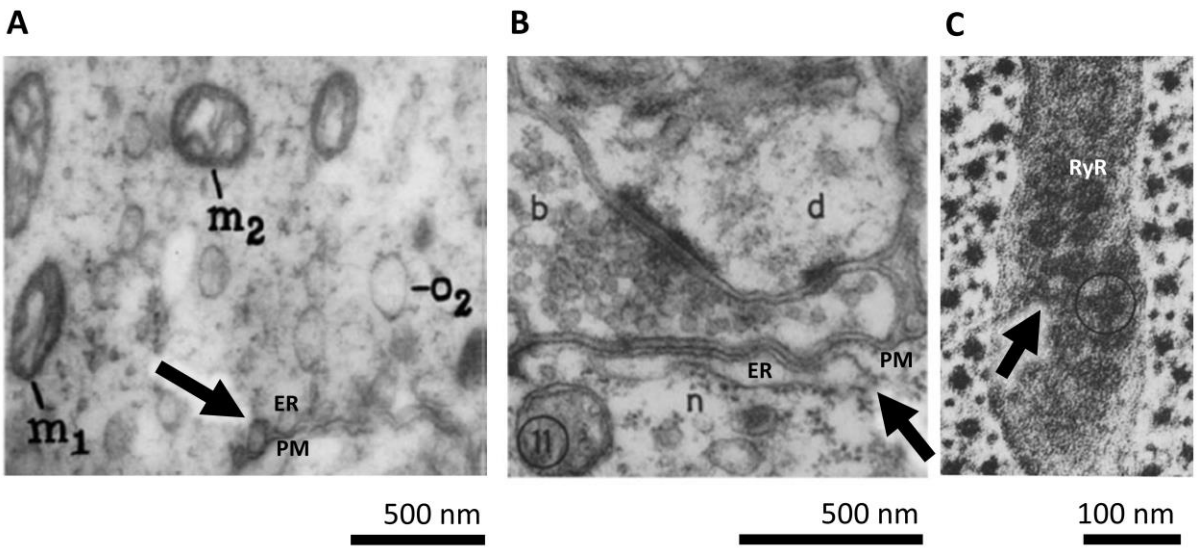

Figure 1: ER-PM MCS visualized by classical EM. (A) One of the first images of these structures ever published [6], showing a section through a rat spermatogonium that includes mitochondria (m1, m2), and ER (o2). The arrow points to ER-PM MCS. (B) First systematic characterization of ER-PM MCS in neurons [7]. The image shows a synaptic bouton (b) forming a synapse with a dendrite (d). An extended ER-PM MCS (arrow) can be seen in an adjacent neurite (n). (C) Grazing section of a triad junction in fish skeletal muscle showing a checkerboard pattern of RyRs (arrow) [26].

Figure 2

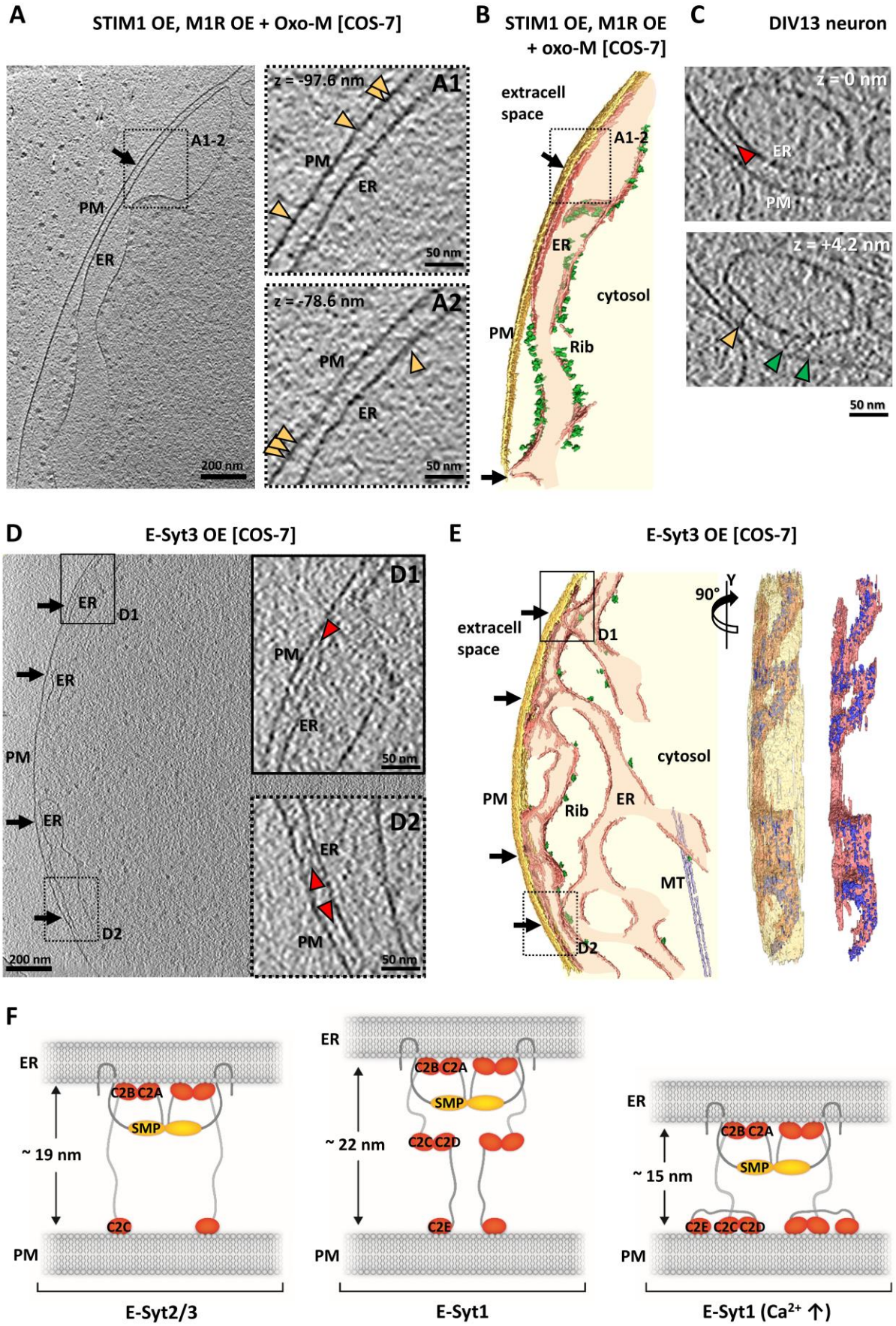
A
STIM1 OE, M1R OE + Oxo-M [COS-7]
A1-2
PM
ER
200 nm
z = -97.6 nm
A1
PM
ER
50 nm
z = -78.6 nm
A2
PM
ER
50 nm
B
STIM1 OE, M1R OE
+ oxo-M [COS-7]
extracell
space
A1-2
ER
cytosol
PM
Rib
C
DIV13 neuron
z = 0 nm
ER
PM
z = +4.2 nm
50 nm
D
E-Syt3 OE [COS-7]
ER
D1
ER
PM
ER
D2
200 nm
D1
PM
ER
50 nm
D2
ER
PM
50 nm
E
E-Syt3 OE [COS-7]
extracell
space
D1
cytosol
PM
Rib
ER
MT
D2
90°
Y
F
ER
C2B C2A
SMP
~ 19 nm
C2C
PM
E-Syt2/3
ER
C2B C2A
SMP
~ 22 nm
C2C C2D
C2E
PM
E-Syt1
ER
C2B C2A
SMP
~ 15 nm
C2E C2C C2D
PM
E-Syt1 (Ca2+ ↑)

Figure 2: ER-PM MCS visualized by cryo-ET [34]. (A) Tomographic slice of a COS-7 cell overexpressing STIM1, the muscarinic receptor M1R and stimulated by 10 µM of the agonist oxotremorine M (STIM1 OE, M1R OE + Oxo-M). The arrow points to an extended ER-PM MCS. In the insets filaments (yellow arrowheads) bridging the ER and PM can be seen. The dotted line on the frame indicates insets showing tomographic slices at different z height than the main panel (B) Surface rendering of (A) showing PM in gold, ER in pink and ribosomes (rib) in green. (C) Tomographic slices of an ER-PM MCS in an untransfected mouse neuron upon 13 days in culture (DIV 13 neuron) showing different types of densities between the ER and the PM: E-Syt-like intermediate density parallel to the membranes (red arrowhead), STIM-like filaments perpendicular to the membranes (yellow arrowhead) and other tethers of unidentified morphology (green arrowheads). (D) Tomographic slice of a COS-7 cell overexpressing E-Syt3 (E-Syt3 OE). Multiple ER-PM MCS are marked by arrows. In the inset, the intermediate density layer between ER and PM is marked by red arrowheads. (E) Left: surface rendering of (D) showing PM in gold, ER in pink, ribosomes (rib) in green and a microtubule (MT) in light blue. Middle and right: en-face view of the ER-PM MCS showing a semi-transparent PM (middle) or no PM (right). The dark blue structures represent the intermediate density layer covering an extended surface of the MCS. (F) Schematic interpretation the cryo-ET data recorded in cells overexpressing different E-Syts. The cartoon is to scale. (Left) In E-Syt2/3-mediated ER-PM MCS E-Syts likely homo/heterodimerize via their SMP domains, the C2A and C2B domains of E-Syt3 may bind the ER membrane and the C2C domain binds PM PI(4, 5)P_2, thereby tethering the ER to the PM [42, 44]. (Middle) The situation is similar in E-Syt1-mediated contacts at resting cytosolic Ca^{2+} concentration, but the two additional C2 domains result in additional ER-PM spacing. (Right) Elevation of cytosolic Ca^{2+} in E-Syt1-mediated contacts results in shortening of the ER-PM distance, likely reflecting the Ca^{2+}-dependent PM binding of the C2C domain of E-Syt1 [42, 43]. Tomographic slices are 2.7 nm thick.

References

1. Elbaz, Y. and M. Schuldiner (2011) *Staying in touch: the molecular era of organelle contact sites.* Trends Biochem Sci, 36(11), p. 616-23.
2. Helle, S.C., G. Kanfer, K. Kolar, A. Lang, A.H. Michel, and B. Kornmann (2013) *Organization and function of membrane contact sites.* Biochim Biophys Acta, 1833(11), p. 2526-41.
3. Levine, T. and C. Loewen (2006) *Inter-organelle membrane contact sites: through a glass, darkly.* Curr Opin Cell Biol, 18(4), p. 371-8.
4. Carrasco, S. and T. Meyer (2011) *STIM proteins and the endoplasmic reticulum-plasma membrane junctions.* Annu Rev Biochem, 80(1), p. 973-1000.
5. Henne, W.M., J. Liou, and S.D. Emr (2015) *Molecular mechanisms of inter-organelle ER-PM contact sites.* Curr Opin Cell Biol, 35, p. 123-30.
6. Palade, G.E. (1955) *Studies on the endoplasmic reticulum. II. Simple dispositions in cells in situ.* J Biophys Biochem Cytol, 1(6), p. 567-82.
7. Rosenbluth, J. (1962) *Subsurface Cisterns and Their Relationship to the Neuronal Plasma Membrane.* J Cell Biol, 13(3), p. 405-421.
8. Franzini-Armstrong, C. and K.R. Porter (1964) *Sarcolemmal Invaginations Constituting the T System in Fish Muscle Fibers.* J Cell Biol, 22, p. 675-96.
9. Asano, S., B.D. Engel, and W. Baumeister (2015) *In Situ Cryo-Electron Tomography: A Post-Reductionist Approach to Structural Biology.* J Mol Biol.
10. Porter, K.R. and G.E. Palade (1957) *Studies on the endoplasmic reticulum. III. Its form and distribution in striated muscle cells.* J Biophys Biochem Cytol, 3(2), p. 269-300.
11. Rossi, A.E. and R.T. Dirksen (2006) *Sarcoplasmic reticulum: the dynamic calcium governor of muscle.* Muscle Nerve, 33(6), p. 715-31.
12. Bers, D.M. (2002) *Cardiac excitation-contraction coupling.* Nature, 415(6868), p. 198-205.
13. Franzini-Armstrong, C. and A.O. Jorgensen (1994) *Structure and development of E-C coupling units in skeletal muscle.* Annu Rev Physiol, 56(1), p. 509-34.
14. Kuo, I.Y. and B.E. Ehrlich (2015) *Muscling in on the ryanodine receptor.* Nat Struct Mol Biol, 22(2), p. 106-7.
15. Santulli, G. and A.R. Marks (2015) *Essential Roles of Intracellular Calcium Release Channels in Muscle, Brain, Metabolism, and Aging.* Curr Mol Pharmacol, 8(2), p. 206-22.
16. Lee, K.S., E. Marban, and R.W. Tsien (1985) *Inactivation of calcium channels in mammalian heart cells: joint dependence on membrane potential and intracellular calcium.* J Physiol, 364, p. 395-411.
17. Lanner, J.T., D.K. Georgiou, A.D. Joshi, and S.L. Hamilton (2010) *Ryanodine receptors: structure, expression, molecular details, and function in calcium release.* Cold Spring Harb Perspect Biol, 2(11), p. a003996.
18. Eggermann, E., I. Bucurenciu, S.P. Goswami, and P. Jonas (2012) *Nanodomain coupling between Ca(2)(+) channels and sensors of exocytosis at fast mammalian synapses.* Nat Rev Neurosci, 13(1), p. 7-21.
19. Dolmetsch, R. (2003) *Excitation-transcription coupling: signaling by ion channels to the nucleus.* Sci STKE, 2003(166), p. PE4.
20. Berkefeld, H., C.A. Sailer, W. Bildl, V. Rohde, J.O. Thumfart, S. Eble, N. Klugbauer, E. Reisinger, J. Bischofberger, D. Oliver, H.G. Knaus, U. Schulte, and B. Fakler (2006) *BKCa-Cav channel complexes mediate rapid and localized Ca2+-activated K+ signaling.* Science, 314(5799), p. 615-20.
21. Takeshima, H., S. Komazaki, M. Nishi, M. Iino, and K. Kangawa (2000) *Junctophilins: a novel family of junctional membrane complex proteins.* Mol Cell, 6(1), p. 11-22.
22. Scriven, D.R., P. Asghari, and E.D. Moore (2013) *Microarchitecture of the dyad.* Cardiovasc Res, 98(2), p. 169-76.
23. Soeller, C. and D. Baddeley (2013) *Super-resolution imaging of EC coupling protein distribution in the heart.* J Mol Cell Cardiol, 58, p. 32-40.

24. Hayashi, T., M.E. Martone, Z. Yu, A. Thor, M. Doi, M.J. Holst, M.H. Ellisman, and M. Hoshijima (2009) *Three-dimensional electron microscopy reveals new details of membrane systems for Ca2+ signaling in the heart.* J Cell Sci, 122(Pt 7), p. 1005-13.
25. Baddeley, D., I.D. Jayasinghe, L. Lam, S. Rossberger, M.B. Cannell, and C. Soeller (2009) *Optical single-channel resolution imaging of the ryanodine receptor distribution in rat cardiac myocytes.* Proc Natl Acad Sci U S A, 106(52), p. 22275-80.
26. Ferguson, D.G., H.W. Schwartz, and C. Franzini-Armstrong (1984) *Subunit structure of junctional feet in triads of skeletal muscle: a freeze-drying, rotary-shadowing study.* J Cell Biol, 99(5), p. 1735-42.
27. Wagenknecht, T., C.E. Hsieh, B.K. Rath, S. Fleischer, and M. Marko (2002) *Electron tomography of frozen-hydrated isolated triad junctions.* Biophys J, 83(5), p. 2491-501.
28. Renken, C., C.E. Hsieh, M. Marko, B. Rath, A. Leith, T. Wagenknecht, J. Frank, and C.A. Mannella (2009) *Structure of frozen-hydrated triad junctions: a case study in motif searching inside tomograms.* J Struct Biol, 165(2), p. 53-63.
29. Prakriya, M. and R.S. Lewis (2015) *Store-Operated Calcium Channels.* Physiol Rev, 95(4), p. 1383-436.
30. Hooper, R. and J. Soboloff (2015) *STIMATE reveals a STIM1 transitional state.* Nat Cell Biol, 17(10), p. 1232-4.
31. Hogan, P.G. (2015) *The STIM1-ORAI1 microdomain.* Cell Calcium, 58(4), p. 357-67.
32. Orci, L., M. Ravazzola, M. Le Coadic, W.W. Shen, N. Demaurex, and P. Cosson (2009) *STIM1-induced precortical and cortical subdomains of the endoplasmic reticulum.* Proc Natl Acad Sci U S A, 106(46), p. 19358-62.
33. Wu, M.M., J. Buchanan, R.M. Luik, and R.S. Lewis (2006) *Ca2+ store depletion causes STIM1 to accumulate in ER regions closely associated with the plasma membrane.* J Cell Biol, 174(6), p. 803-13.
34. Fernandez-Busnadiego, R., Y. Saheki, and P. De Camilli (2015) *Three-dimensional architecture of extended synaptotagmin-mediated endoplasmic reticulum-plasma membrane contact sites.* Proc Natl Acad Sci U S A, 112(16), p. E2004-13.
35. Moser von Filseck, J., B. Mesmin, J. Bigay, B. Antonny, and G. Drin (2014) *Building lipid 'PIPelines' throughout the cell by ORP/Osh proteins.* Biochem Soc Trans, 42(5), p. 1465-70.
36. Mesmin, B., J. Bigay, J. Moser von Filseck, S. Lacas-Gervais, G. Drin, and B. Antonny (2013) *A Four-Step Cycle Driven by PI(4)P Hydrolysis Directs Sterol/PI(4)P Exchange by the ER-Golgi Tether OSBP.* Cell, 155(4), p. 830-843.
37. Moser von Filseck, J., A. Copic, V. Delfosse, S. Vanni, C.L. Jackson, W. Bourguet, and G. Drin (2015) *Phosphatidylserine transport by ORP/Osh proteins is driven by phosphatidylinositol 4-phosphate.* Science, 349(6246), p. 432-6.
38. Chung, J., F. Torta, K. Masai, L. Lucast, H. Czapla, L.B. Tanner, P. Narayanaswamy, M.R. Wenk, F. Nakatsu, and P. De Camilli (2015) *PI4P/phosphatidylserine countertransport at ORP5- and ORP8-mediated ER-plasma membrane contacts.* Science, 349(6246), p. 428-32.
39. Stefan, C.J., A.G. Manford, D. Baird, J. Yamada-Hanff, Y. Mao, and S.D. Emr (2011) *Osh proteins regulate phosphoinositide metabolism at ER-plasma membrane contact sites.* Cell, 144(3), p. 389-401.
40. Chang, C.L., T.S. Hsieh, T.T. Yang, K.G. Rothberg, D.B. Azizoglu, E. Volk, J.C. Liao, and J. Liou (2013) *Feedback regulation of receptor-induced Ca2+ signaling mediated by E-Syt1 and Nir2 at endoplasmic reticulum-plasma membrane junctions.* Cell Rep, 5(3), p. 813-25.
41. Manford, A.G., C.J. Stefan, H.L. Yuan, J.A. Macgurn, and S.D. Emr (2012) *ER-to-plasma membrane tethering proteins regulate cell signaling and ER morphology.* Dev Cell, 23(6), p. 1129-40.
42. Giordano, F., Y. Saheki, O. Idevall-Hagren, S.F. Colombo, M. Pirruccello, I. Milosevic, Elena O. Gracheva, Sviatoslav N. Bagriantsev, N. Borgese, and P. De Camilli (2013) *PI(4,5)P2-*

Dependent and Ca2+-Regulated ER-PM Interactions Mediated by the Extended Synaptotagmins. Cell, 153(7), p. 1494-1509.
43. Idevall-Hagren, O., A. Lu, B. Xie, and P. De Camilli (2015) *Triggered Ca2+ influx is required for extended synaptotagmin 1-induced ER-plasma membrane tethering.* EMBO J, 34(17), p. 2291-305.
44. Schauder, C.M., X. Wu, Y. Saheki, P. Narayanaswamy, F. Torta, M.R. Wenk, P. De Camilli, and K.M. Reinisch (2014) *Structure of a lipid-bound extended synaptotagmin indicates a role in lipid transfer.* Nature, 510(7506), p. 552-5.
45. Toulmay, A. and W.A. Prinz (2012) *A conserved membrane-binding domain targets proteins to organelle contact sites.* J Cell Sci, 125(Pt 1), p. 49-58.
46. Stiber, J.A. and P.B. Rosenberg (2011) *The role of store-operated calcium influx in skeletal muscle signaling.* Cell Calcium, 49(5), p. 341-9.
47. Maleth, J., S. Choi, S. Muallem, and M. Ahuja (2014) *Translocation between PI(4,5)P2-poor and PI(4,5)P2-rich microdomains during store depletion determines STIM1 conformation and Orai1 gating.* Nat Commun, 5, p. 5843.
48. Hsieh, C., T. Schmelzer, G. Kishchenko, T. Wagenknecht, and M. Marko (2014) *Practical workflow for cryo focused-ion-beam milling of tissues and cells for cryo-TEM tomography.* J Struct Biol, 185(1), p. 32-41.